

Compensation for Stochastic Error of Gyros in a Dual-axis Rotational Inertial Navigation System

Zhichao Zheng¹, Songlai Han², Jin Yue³ and Linglong Yuan³

¹(*Wuhan National Laboratory for Optoelectronics, School of Optoelectronic Science and Engineering, Huazhong University of Science and Technology, Wuhan 430074, People's Republic of China*)

²(*College of Optoelectronic Science and Engineering, National University of Defense Technology, Changsha, Hunan 410073, People's Republic of China*)

³(*Huazhong Institute of Optoelectronics Technology, Wuhan 430074, People's Republic of China*)

(E-mail: zhengzhichao116@126.com)

A dual-axis rotational Inertial Navigation System (INS) has received wide attention in recent years because of high performance and low cost. However, some errors of inertial sensors such as stochastic errors are not averaged out automatically during navigation. Therefore a Twice Position-fix Reset (TPR) method is provided to enhance accuracy of a dual-axis rotational INS by compensating stochastic errors. According to characteristics of an azimuth error introduced by stochastic errors of an inertial sensor in the dual-axis rotational INS, both an azimuth error and a radial-position error are much better corrected by the TPR method based on an optimised error propagation equation. As a result, accuracy of the dual-axis rotational INS is prominently enhanced by the TPR method, as is verified by simulations and field tests.

KEYWORDS

1. Inertial Navigation. 2. Inertial Measurement Unit. 3. Position-fix Reset. 4. Stochastic Error.

Submitted: 16 September 2014. Accepted: 16 June 2015. First published online: 6 July 2015.

1. INTRODUCTION. A dual-axis rotational Inertial Navigation System (INS) has been developed from Strapdown Inertial Sensing Unit Rotation (SISUR) technology (Fincke, 1978), which averages out drifts by rotating an Inertial Measurement Unit (IMU) about its azimuth and roll axes every few minutes. With the benefits of high performance and low cost, the dual-axis rotational INS is widely fitted to naval ships and submarines of the North Atlantic Treaty Organization (NATO) including the United States (Titterton and Weston, 2004; Levinson and Majure, 1987).

To enhance accuracy of the dual-axis rotational INS, many special techniques have been discussed in recent years. Levinson et al. (1980) introduced a dual-axis rotation scheme technique, self-calibration and position-fix reset (Levinson and Majure,

1987). Yuan et al. (2012) proposed a 16-position rotation scheme, where all the gyro drifts can be compensated without introducing extra system error accumulations. Yin et al. (2012) described some important issues of the dual-axis rotational INS, including error propagation characteristics and rotation scheme design. Song et al. (2013) discussed errors caused by a dual-axis turntable.

The schemes and techniques mentioned above have solved some practical problems of the dual-axis rotational INS; however, to achieve higher accuracy, there are some important aspects that need to be investigated:

- *Position-fix reset.* For a general INS, stochastic errors of gyros introduce a position error and an azimuth error. Only the position error can be compensated by using a conventional position-fix reset method (Levinson and Majure, 1987). In fact, by optimising an attitude error model, not only the position error but also the azimuth error can be compensated in a dual-axis rotational INS.
- *16-position rotation scheme.* Results of theoretical analysis and simulation indicate that a 16-position rotation scheme is quite suitable for a dual-axis rotational INS, because all the gyro drifts can be compensated without introducing extra system error accumulations. Therefore, a performance advantage of the 16-position rotation scheme can be experimentally demonstrated by performing this scheme on a dual-axis rotational INS.

Considering the aforementioned demands, this paper contains two main contributions. First, a dual-axis rotational INS is designed for experimentally demonstrating the results of theoretical analysis. Second, a Twice Position-fix Reset (TPR) method, which corrects both the position error and the azimuth error introduced by the stochastic errors, is proposed.

The rest of this paper is organised as follows: the design of the rotational INS is described in Section 2 and an error model of a dual-axis rotational INS is provided in Section 3. The TPR method is provided in Section 4, results and analysis are shown in Section 5 and concluding remarks are in Section 6.

2. DESIGN OF A DUAL-AXIS ROTATIONAL INERTIAL NAVIGATION SYSTEM. An overall view and a functional diagram of the designed dual-axis rotational INS are shown in Figure 1 and in Figure 2, respectively. In the designed dual-axis rotational INS, a navigation grade IMU is developed using three dithered ring laser gyroscopes ($0.005^\circ \text{ h}^{-1}$), three quartz accelerometers ($100 \mu\text{g}$), a low-cost dual-axis turntable (18 arc-sec in 1σ) and a shock isolation system. A turntable is designed by using two orthogonal gimbals, including an azimuth (inner) gimbal and a roll (outer) gimbal. On rotors of the gimbals, two electrical torques and two angle encoders are mounted to control rotations. In addition, two slip-rings are mounted on the gimbals to support cables connecting inertial sensors and outer circuits.

3. ERROR MODEL OF A DUAL-AXIS ROTATIONAL INS. Since the dual-axis rotational INS evolves from a strapdown INS, its error propagation equations should be the same as those of a general strapdown INS (Yuan et al., 2012). Derivation of the INS error propagation equations has two equivalent approaches: a phi-angle-based approach and a psi-angle-based approach (Goshen-Meskin and Bar-Itzhack, 1992; Benson, 1975). In this work, we adopt the psi-angle error model

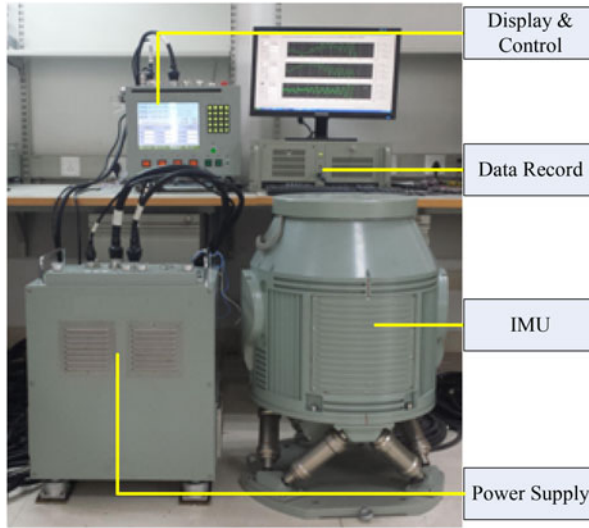


Figure 1. An overall view of the designed dual-axis rotational INS.

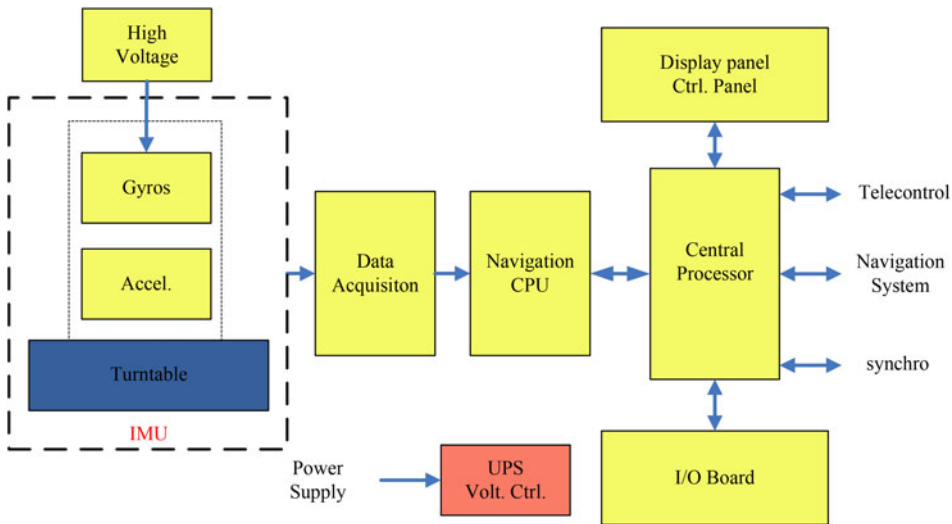


Figure 2. A functional diagram of the designed dual-axis rotational INS.

to express error propagation characteristics of the dual-axis rotational INS.

$$\dot{\psi}^n = -(\omega_{ie}^n + \omega_{en}^n) \times \psi^n - C_b^n \epsilon^b \tag{1}$$

$$\begin{aligned} \delta \dot{\mathbf{v}}^n &= \mathbf{f}^n \times \psi^n - (2\omega_{ie}^n + \omega_{en}^n) \times \delta \mathbf{v}^n - (2\delta \omega_{ie}^n + \delta \omega_{en}^n) \\ &\times \mathbf{v}^n + \delta \mathbf{g}^n + C_b^n \nabla^b \end{aligned} \tag{2}$$

$$\delta \dot{\mathbf{r}}^n = -\omega_{en}^n \times \delta \mathbf{r}^n + \delta \mathbf{v}^n \tag{3}$$

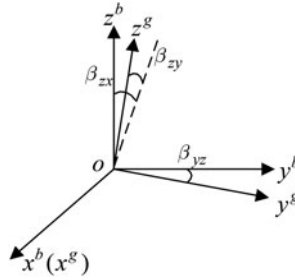


Figure 3. Definition of the body frame (*b* frame).

where *n*, *b*, *i* and *e* represent a navigation frame, a body frame, an inertial frame and an Earth frame, respectively. Superscripts of the vectors denote frames to which the vectors are projected. $\boldsymbol{\psi}^n$, $\delta\mathbf{v}^n$ and $\delta\mathbf{r}^n$ represent a psi-angle error (attitude error), a velocity error and a position error, respectively. \mathbf{f}^n is a specific force, $\boldsymbol{\omega}$ represents an angular rate, and $\delta\boldsymbol{\omega}$ represents an angular rate error, the symbol ‘ \times ’ denotes taking cross product of two vectors. \mathbf{C}_b^n represents a direction cosine matrix (DCM) of the *n*-frame with respect to the *b*-frame. $\boldsymbol{\varepsilon}^b$ and Δ^b denote a gyroscope drift error and an accelerometer drift error, respectively. Expanded forms of $\boldsymbol{\varepsilon}^b$ and Δ^b are given in following equations (Titterton and Weston, 2004).

$$\boldsymbol{\varepsilon}^b = \mathbf{b}_g + \mathbf{S}_g\boldsymbol{\omega}^b + \mathbf{N}_g\boldsymbol{\omega}^b + \mathbf{K}_g\mathbf{f}^b + \mathbf{v}_g \tag{4}$$

$$\nabla^b = \mathbf{b}_a + \mathbf{S}_a\mathbf{f}^b + \mathbf{N}_a\mathbf{f}^b + \mathbf{v}_a \tag{5}$$

where \mathbf{b}_g and \mathbf{b}_a are constant biases, \mathbf{S}_g and \mathbf{S}_a are scale factor error matrices, \mathbf{N}_g and \mathbf{N}_a represent misalignment error matrices, $\boldsymbol{\omega}^b$ is the angular rate projected to the body frame, \mathbf{f}^b is a specific force projected to the body frame, \mathbf{K}_g is a *g*-dependent bias coefficient matrix, \mathbf{v}_g and \mathbf{v}_a denote stochastic errors.

The body frame *b* (as shown in Figure 3), which is an orthogonal coordinate frame associated with the gyro’s sensitivity axes, is defined as follows: x^b coincides with the x^g gyro sensitivity axis, y^b lies in the $y^g x^g$ plane and z^b constitutes a right-handed orthogonal frame with x^b , y^b .

As the misalignment errors are small angles, the misalignment error matrix of gyros can be written as:

$$\mathbf{N}_g = \begin{bmatrix} 1 & 0 & 0 \\ y^g \cdot x^b & y^g \cdot y^b & 0 \\ z^g \cdot x^b & z^g \cdot y^b & z^g \cdot z^b \end{bmatrix} = \begin{bmatrix} 1 & 0 & 0 \\ -\beta_{yz} & 1 & 0 \\ -\beta_{zy} & -\beta_{zx} & 1 \end{bmatrix} \tag{6}$$

Similarly, the accelerometer sensitivity axes are not associated with the gyros’ sensitivity axes, the misalignment error matrix of accelerometer can be written as (Song, 2013):

$$\mathbf{N}_a = \begin{bmatrix} 1 & \eta_{xz} & -\eta_{xy} \\ -\eta_{yz} & 1 & -\eta_{yx} \\ \eta_{zy} & -\eta_{zx} & 1 \end{bmatrix} \tag{7}$$

4. TWICE POSITION-FIX RESET (TPR) METHOD. Position-fix reset is a general technique to deal with a position error introduced by stochastic errors of gyros, where a position of an INS is reset when position information is provided. The stochastic errors of gyros introduce both an azimuth error and a position error. However, the azimuth error is usually ignored in a conventional position-fix reset method (Bona and Smay, 1966).

In this section, the characteristic of the azimuth error introduced by stochastic errors of gyros is studied, followed by a TPR method provided for compensating stochastic errors of a dual-axis rotational INS. Comparing with the conventional position-fix reset method, the main novelty and advantage of the TPR method are that both the azimuth error and the position error introduced by the stochastic errors of gyros are estimated and corrected.

4.1. *Characteristics of the Azimuth Error Introduced by Stochastic Errors of Gyros.* As mentioned above in Section 3, the phi-angle-based approach and the psi-angle-based approach are two equivalent approaches for derivation of error equations of an INS. The relationship between them is shown as follows (Goshen-Meskin, and Bar-Itzhack, 1992):

$$\Phi^n = \delta\theta^n + \psi^n \tag{8}$$

where Φ is the phi-angle error, and ψ is the psi-angle error. $\delta\theta$ is the position error, which can be written as:

$$\delta\theta^n = [\delta\theta_x \quad \delta\theta_y \quad \delta\theta_z]^T = [-\delta L \quad \delta\lambda \cos L \quad \delta\lambda \sin L]^T \tag{9}$$

where L represents a local latitude, δL and $\delta\lambda$ represent a latitude error and a longitude error, respectively.

With calibration, the characteristics of deterministic errors, such as the g-dependent biases, the scale factor errors and the misalignment errors, can be well investigated (Syed et al., 2007; Nieminen et al., 2010; Fong et al., 2008; Zhang et al., 2010; Li et al., 2012). The sensor error model can be simplified as follows:

$$\epsilon^b = \mathbf{b}_g + \mathbf{v}_g \tag{10}$$

$$\nabla^b = \mathbf{b}_a + \mathbf{v}_a \tag{11}$$

According to the principles of the dual-axis rotational INS (Levinson and Majure, 1987; Yuan et al., 2012), the items \mathbf{b}_g and \mathbf{b}_a in Equations (4) and (5) can be averaged out, thus the stochastic error introduced by the gyros is the main error source in the dual-axis rotational INS. Thus, Equation (1) can be rewritten as follows:

$$\dot{\psi}^n + \omega_{in}^n \times \psi^n = \mathbf{v}_g \tag{12}$$

For applications to a land vehicle, a ship or a submarine, which lasts for a long term, typically for several days, velocity damping is usually utilised to reduce navigation errors which propagate in a Schuler period, and hence the pitch error and the roll error are greatly attenuated (Gao, 2012). However, the velocity damping is not effective in reducing the azimuth error.

4.2. *The TPR method.* To estimate and correct the azimuth error and the position error introduced by the stochastic errors, we propose an optimised position-fix reset method called Twice Position-fix Reset (TPR). It contains two steps:

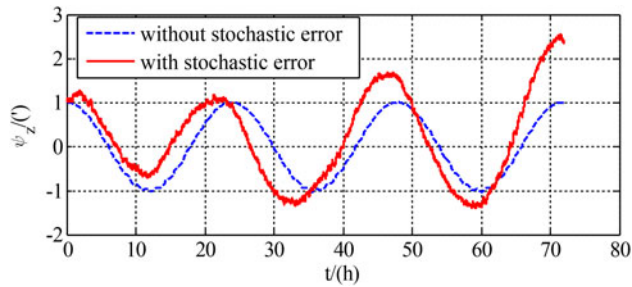


Figure 4. Propagation characteristic of an azimuth error of the psi-angle.

- a) Reset the position of the INS when first position information is available;
- b) Estimate and correct the azimuth error and reset the position of the INS when second position information is available. The following are the details of the TPR method.

Considering $\omega_{ie}^n \gg \omega_{en}^n$ for low speed vehicles, the psi-angle-based equation in a dual-axis rotational INS can be simplified as:

$$\dot{\psi}^n + \omega_{ie}^n \times \psi^n = \mathbf{v}_g \quad (13)$$

where $\omega_{ie}^n = [0 \ \Omega \cos L \ \Omega \sin L]^T$, Ω is the Earth's rate. From Equation (13), the characteristic period of psi-angle is:

$$T_0 = \frac{2\pi}{|\omega_{ie}^n|} = \frac{2\pi}{\Omega} \quad (14)$$

In general, the stochastic errors of gyros slowly and accumulatively affect the propagation characteristic of the psi-angle in the characteristic period ($T_0 = 24$ hours), so the stochastic errors of the gyros need to be compensated in a long-term mission. A general azimuth error of the psi-angle propagates as shown in Figure 4.

The interval between the two resets is about 4–6 hours, which is much shorter than the characteristic period. As shown in Figure 4, within the initial 4–6 hours, the accumulated effect caused by the stochastic error is still limited. Therefore, within the interval between the two resets, the psi-angle with stochastic errors may be fitted by the psi-angle without considering the stochastic errors.

For example, a reset is performed at the 40th hour, and the fitting is performed between the 40th hour and the 46th hour. As shown in Figure 5, the curve of an azimuth error with a stochastic error is fit with the curve of the azimuth error without considering the stochastic error. The fitting is accurate enough for the short interval.

According to Equation (14) for the psi-angle with the stochastic errors, Equation (15) is obtained for the psi-angle without considering the stochastic error, which can be written as follows:

$$\dot{\psi}^n + \omega_{ie}^n \times \psi^n = 0 \quad (15)$$

Because the latitude varies as vehicle moves, the ω_{ie}^n is not constant. To solve Equation (15), a right-handed frame called s-frame is defined. The s-frame has its origin at the

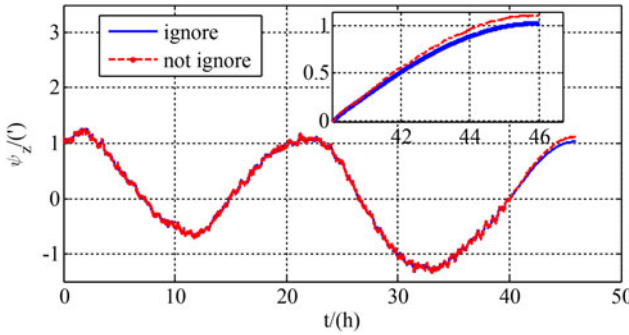


Figure 5. Fitting an azimuth error by ignoring the stochastic error between the 40th hour and the 46th hour.

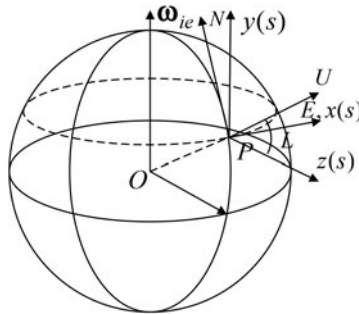


Figure 6. The s-frame and the navigation frame.

location of the navigation system, and its x-axis and y-axis align with the directions of east and the Earth axis. The s-frame can be obtained by rotating the navigation frame by an angle (Latitude) about the x-axes. Figure 6 shows the relationship between the s-frame and the navigation frame.

The DCM of the navigation frame with respect to the s-frame is:

$$C_n^s = \begin{bmatrix} 1 & 0 & 0 \\ 0 & \cos L & \sin L \\ 0 & -\sin L & \cos L \end{bmatrix} \tag{16}$$

According to the DCM C_n^s , the psi-angle in the s-frame can be written as:

$$\Psi^s = C_n^s \Psi^n \tag{17}$$

Since s-frame is stationary respect to the n-frame, $\omega_{ns}^s = 0$. Substituting Ψ^n in Equation (15) with Ψ^s , the psi-angle-based equation in the s-frame gives:

$$\begin{cases} \dot{\Psi}_x^s + \Omega \cdot \Psi_z^s = 0 \\ \dot{\Psi}_y^s = 0 \\ \dot{\Psi}_z^s - \Omega \cdot \Psi_x^s = 0 \end{cases} \tag{18}$$

The analytical solutions of Equation (18) are given by:

$$\Psi^s(t) = \mathbf{T}(t, t_0) \cdot \Psi^s(t_0) \quad (19)$$

With

$$\mathbf{T}(t, t_0) = \begin{bmatrix} \cos \Omega(t - t_0) & 0 & -\sin \Omega(t - t_0) \\ 0 & 1 & 0 \\ \sin \Omega(t - t_0) & 0 & \cos \Omega(t - t_0) \end{bmatrix} \quad (20)$$

According to the analysis in Subsection 4.1, the pitch error and the roll error can be greatly reduced by velocity damping, thus, it is sufficiently precise to assume the pitch error and the roll error are zero during a period of the two observations. Thus, Equation (8) can be written as:

$$\begin{cases} \phi_x^n = \delta\theta_x^n + \psi_x^n = 0 \\ \phi_y^n = \delta\theta_y^n + \psi_y^n = 0 \\ \phi_z^n = \delta\theta_z^n + \psi_z^n \end{cases} \quad (21)$$

Substituting Equations (8), (9), and (18) into Equations (21) yields:

$$\begin{bmatrix} \delta L \\ \delta\lambda \\ \phi_z^n \end{bmatrix} = \begin{bmatrix} 1 & 0 & 0 \\ 0 & -1 & \tan L \\ 0 & 0 & \sec L \end{bmatrix} \begin{bmatrix} \psi_x^s \\ \psi_y^s \\ \psi_z^s \end{bmatrix} \quad (22)$$

By the first position information, Equation (19) can be rearranged as a first position-fix reset equation:

$$\begin{bmatrix} \delta L(t_1) \\ \delta\lambda(t_1) \\ \phi_z^n(t_1) \end{bmatrix} = \begin{bmatrix} 1 & 0 & 0 \\ 0 & -1 & \tan L \\ 0 & 0 & \sec L \end{bmatrix} \begin{bmatrix} \psi_x^s(t_1) \\ \psi_y^s(t_1) \\ \psi_z^s(t_1) \end{bmatrix} \quad (23)$$

Similarly, a second position-fix reset equation is given by:

$$\begin{bmatrix} \delta L(t_2) \\ \delta\lambda(t_2) \\ \phi_z^n(t_2) \end{bmatrix} = \begin{bmatrix} 1 & 0 & 0 \\ 0 & -1 & \tan L \\ 0 & 0 & \sec L \end{bmatrix} \begin{bmatrix} \psi_x^s(t_2) \\ \psi_y^s(t_2) \\ \psi_z^s(t_2) \end{bmatrix} \quad (24)$$

Following Equations (23) and (24), the relationship between the two observations can be written as:

$$\begin{cases} \psi_x^s(t_2) = \cos \Omega(t_2 - t_1) \cdot \psi_x^s(t_1) - \sin \Omega(t_2 - t_1) \cdot \psi_z^s(t_1) \\ \psi_z^s(t_2) = \sin \Omega(t_2 - t_1) \cdot \psi_x^s(t_1) + \cos \Omega(t_2 - t_1) \cdot \psi_z^s(t_1) \end{cases} \quad (25)$$

With the second position information, the item of $\psi_x^s(t_2)$ in Equation (24) can be calculated, and the items of $\psi_z^s(t_1)$ and $\psi_z^s(t_2)$ can be given by Equation (25). Substituting $\psi_z^s(t_2)$ in Equation (24), we can get the azimuth error $\phi_z^n(t_2)$.

As stated above, there are three assumptions: a) pitch error and roll error are zero; b) the constant bias errors of gyros are averaged out; c) $\omega_{ie}^n \gg \omega_{en}^n$. In practice, the assumptions are not satisfied all over the period of position-fix reset, but the TPR method is fine to estimate most parts of the azimuth error for applications with low speed and low manoeuvres, which was verified by simulations (Section 4.3) and field tests (Section 5).

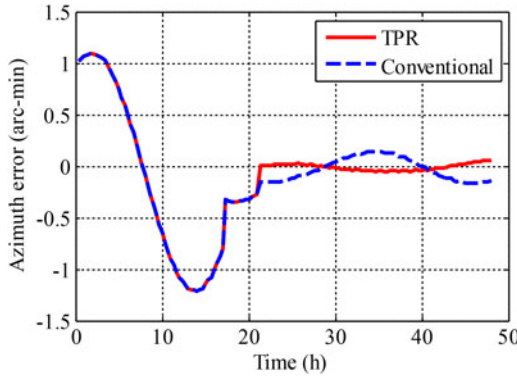


Figure 7. Azimuth errors (phi-angle) with velocity damping by using the TPR method and by using the conventional method.

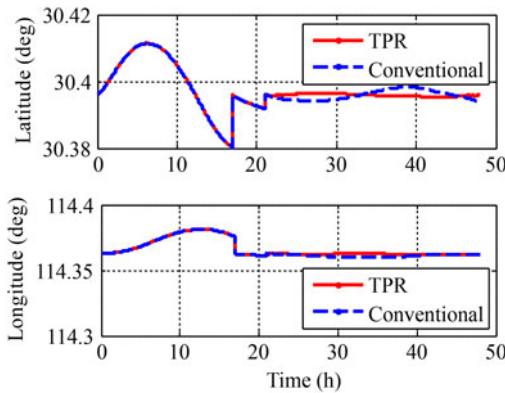


Figure 8. Position outputs with velocity damping by using the TPR method and by using the conventional method.

4.3. *Simulation of the TPR Method.* To verify the advantage of the proposed TPR method, the conventional position-fix reset method and TPR method are both simulated. A stationary simulation is carried out with the following conditions: (1) an initial alignment attitude error is $(0', 0', 1')$, (2) the stochastic error of the gyro is $3 \times 10^{-3} \text{ deg h}^{-1/2}$, the stochastic error of the accelerometer is $20 \mu\text{g Hz}^{-1/2}$, and (3) the twice position-fix resets are carried out at the 17th hour and the 21th hour, respectively, (4) the INS navigates with velocity damping.

Figure 7 shows a comparison of azimuth errors with velocity damping by using the TPR method and by using the conventional position-fix reset method. A comparison of position outputs by using the TPR method and by using the conventional method is shown in Figure 8. Both methods corrected the position error at the 17th hour. At the 21th hour, the azimuth error (phi-angle error) which include the psi-angle error and the position error are compensated by the TPR method, while only the position error is compensated by the conventional position-fix reset method.

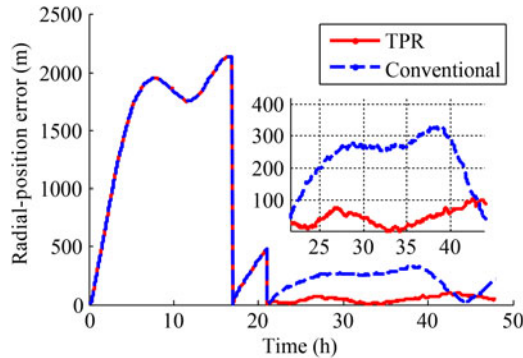


Figure 9. Radial-position errors with velocity damping by using the TPR method and by using the conventional method.

Table 1. Specifications of the designed dual-axis rotational INS.

Characteristics	Description
Output rates	200 Hz
Gyro fixed bias (1σ)	0.005°/h
Gyro stochastic error	0.0007°/h ^{1/2}
Gyro scale factor error	<30 ppm
Gyro misalignment error	<20 arc-sec
Gyro g-dependent bias	0.0001°/h/g
Accel. fixed bias (1σ)	100ug
Accel. stochastic error	50ug / Hz ^{1/2}
Accel. scale factor error	<30 ppm
Accel. misalignment error	<20 arc-sec
Sensor range	Gyros: ±300°/s FS Accel. : ±40 g FS
A/D resolution	16 bits
Supply Voltage	5.0 V, 24 V
Turntable (1σ)	18"

Radial-position errors compensated by the TPR method and by the conventional position-fix reset method are compared in Figure 9. It can be seen that the radial-position error is less than 100 m by using the TPR method, while it is more than 310 m by using the conventional method.

From the comparisons above, both the azimuth error and the radial-position error are significantly better corrected by the TPR method than by a conventional position-fix reset method under same conditions in simulations.

5. FIELD TEST. The TPR method was applied to the designed dual-axis rotational INS mentioned in Section 2 and a field test was carried out to verify the performances. Specifications of the designed dual-axis rotational INS are listed in Table 1.

The trajectory, which is shown in Figure 10, starts from a location at Wuhan (114.3494°E, 30.3947°N) and ended at a location Kaifeng (114.3680°E, 34.7920°N).

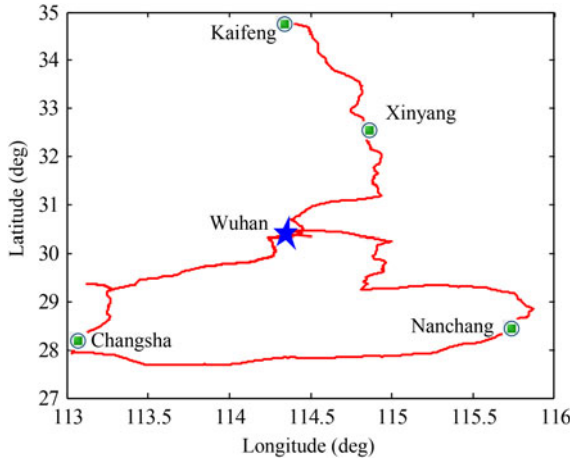


Figure 10. Trajectory of a test run (start position is denoted by a star).

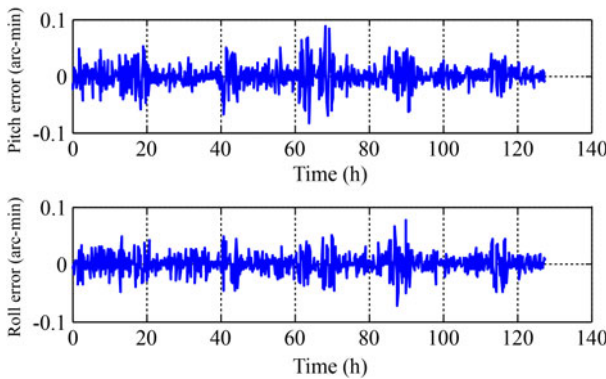


Figure 11. Pitch error and roll error with velocity damping in step (1).

This trajectory involves moderate swings and accelerations. The Global Position System (GPS) signal was continuous and experienced no outages during the 133 hours of the test run. GPS positions were not given to the INS until the position-fix reset was needed at the 72nd hour and the 76th hour during the test. In order to verify the advantage of the proposed TPR method, the vehicle continued to run another 51 hours after the resets.

To evaluate the TPR method, position information from GPS was treated as an external position reference, attitude information resolved by a GPS/INS loose integrated algorithm (Titterton and Weston, 2004) was treated as an external azimuth reference and the pitch, roll reference, and the raw IMU data was recorded in real-time with a frequency of 200 Hz for post-processing.

The procedure, which is used to evaluate the proposed TPR method, includes two steps:

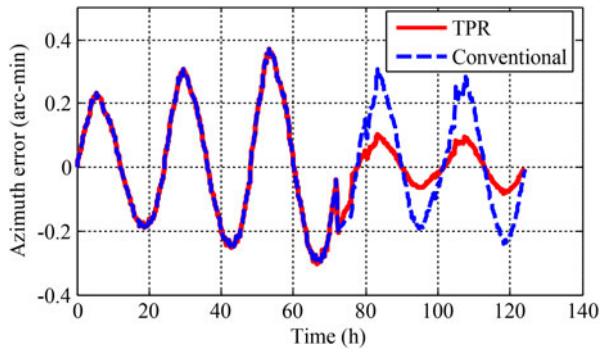


Figure 12. Azimuth errors with velocity damping by using the TPR method and conventional method.

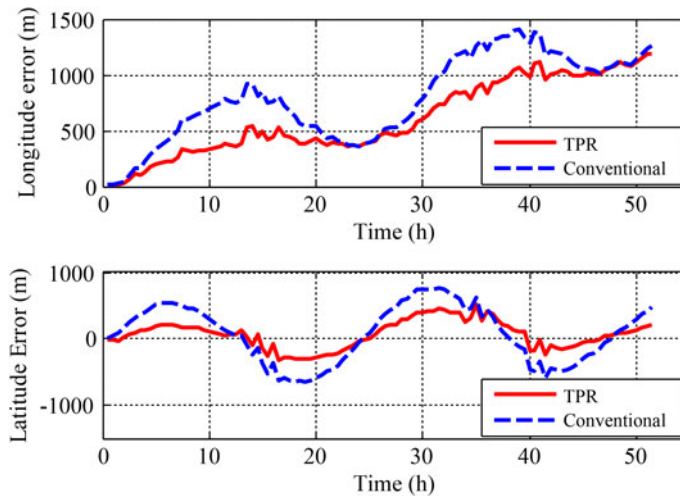


Figure 13. Longitude errors and latitude errors with velocity damping in the latter 51 hours by using the proposed TPR method and by using the conventional position-fix reset method.

- (1) Align the IMU by using a multi-position alignment method and make the system navigate for 127 hours with velocity damping, where the system is reset by using the TPR method at the 72nd hour and the 76th hour during the test;
- (2) Align the IMU by using the multi-position method and make the system navigate for 127 hours with velocity damping, where the system is reset by using the conventional position-fix reset method at the 72nd hour and the 76th hour during the test.

The pitch error and the roll error of the navigation results in step (1) are shown in Figure 11. With velocity damping, both the pitch error and the roll error are less

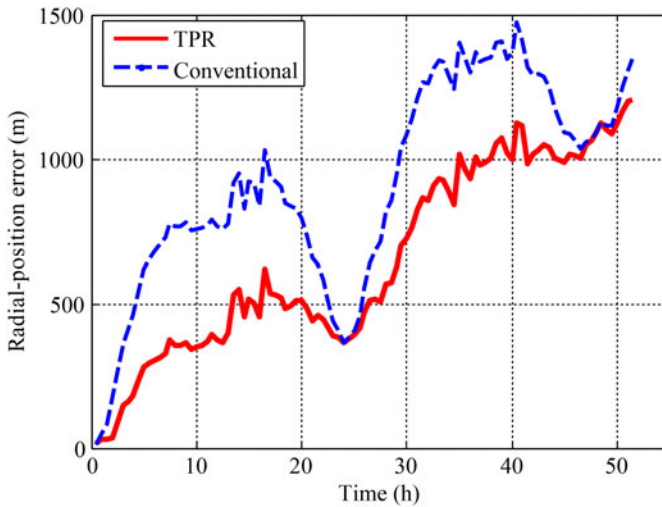


Figure 14. Radial-position errors with velocity damping in the latter 51 hours by using the proposed TPR method and by using the conventional position-fix reset method.

than 0.1 arc-min, thus, it is sufficiently precise to assume the pitch error and the roll error are zero in Equation (19).

The azimuth errors of the navigation results in step (1) and in step (2) are shown in Figure 12. At the 72nd hour, both methods corrected the position error, and at the 76th hour, the azimuth error which include the psi-angle and the position error are compensated by the TPR method, while only the position error is compensated by the conventional position-fix reset method. Thus, the residual azimuth error is less by using the TPR method than by using the conventional position-fix reset method. From Figure 12, it can be seen that the TPR method is fine to estimate the majority of the azimuth errors.

Figure 13 shows comparisons of the longitude error and the latitude error in the latter 51 hours by using the proposed TPR method and by using the conventional position-fix reset method. The comparison of the radial-position error in the latter 51 hours is shown in Figure 14. It can be seen that the radial-position error by using the proposed TPR method is much smaller than that by using the conventional method, which is expected due to the correction of the azimuth error during the twice position-fix resets.

6. CONCLUSION. To enhance accuracy of a dual-axis rotational INS for long-term navigation applications, a Twice Position-fix Reset (TPR) method is proposed in this paper. Specifically, the following contributions have been made:

With calibration methods and 16-position rotation scheme, stochastic errors of the inertial sensors are one of the main residual errors which lead the azimuth error and the position error to be divergent as a function of time. The TPR method is designed to compensate for the stochastic errors by estimating the azimuth error and the position error with two observations.

Field tests indicate that, compared with the conventional approach, the TPR method dramatically improved the performances of the dual-axis rotational INS.

ACKNOWLEDGEMENT

This work is supported in part by National Natural Science Foundation of China (Grant No: 61203199).

REFERENCES

- Benson, D.O., Jr. (1975). A Comparison of Two Approaches to Pure-inertial and Doppler-inertial Error Analysis. *IEEE Transaction on Aerospace and Electronic Systems*, **11**, 447–55.
- Bona, B.E. and Smay, R.J. (1966). Optimum Reset of Ship's Inertial Navigation System. *IEEE Transaction on Aerospace and Electronic Systems*, **2**, 409–414.
- Fincke, W.H. (1978). Strapdown Inertial Sensing Unit Rotation (SISUR): A New Approach to Inertial Navigation. *Position Location and Navigation Symposium*, San Diego, CA.
- Fong, W.T., Ong, S.K. and Nee, A. (2008). Methods for In-field User Calibration of An Inertial Measurement Unit without External Equipment. *Measurement Science and Technology*, **19**, 085202.
- Gao, Z.Y. (2012). *Inertial Navigation System Technology 1st edition* (Beijing:Tsinghua University Press) pp. 270–1.
- Goshen-Meskin, D. and Bar-Itzhack, I.Y. (1992). Unified Approach to Inertial Navigation System Error Modeling. *Journal of Guidance Control Dynamic*, **15**, 648–53.
- Levinson, E. and Majure, R. (1987). Accuracy Enhancement Techniques Applied to The Marine Ring Laser Inertial Navigator (MARLIN). *Navigation*, **34**, 64–86.
- Levinson, E. and San Giovanni, C. (1980). Laser Gyro Potential for Long Endurance Marine Navigation. *IEEE Position Location Navigation Symposium*, Atlantic City, NJ, USA. 115–29.
- Li, Y., Niu, X., Zhang, Q., Zhang, H. and Shi, C. (2012). An in situ Hand Calibration Method Using A Pseudo-observation Scheme for Low-end Inertial Measurement Units. *Measurement Science and Technology*, **23**, 105104.
- Nieminen, T., Kangas, J., Suuriniemi, S. and Kettunen, L. (2010). An Enhanced Multi-position Calibration Method for Consumer-grade Inertial Measurement Units Applied and Tested. *Measurement Science and Technology*, **21**, 105204.
- Song, N., Cai, Q., Yang, G. and Yin, H. (2013). Analysis and Calibration of The Mounting Errors Between Inertial Measurement Unit and Turntable in Dual-axis Rotational Inertial Navigation System. *Measurement Science and Technology*, **24**, 115002.
- Syed, Z.F., Aggarwal, P., Goodall, C., Niu, X. and El-Sheimy, N. (2007). A New Multi-position Calibration Method for MEMS Inertial Navigation Systems. *Measurement Science and Technology*, **18**, 1897–907.
- Titterton, D.H. and Weston, J.L. (2004). *Strapdown Inertial Navigation Technology 2nd edition* (London/Reston, VA: IET/AIAA).
- Yin, H., Yang, G., Song, N., Jiang, R. and Wang, Y. (2012). Error Modulation Scheme Analyzing for Dual-axis Rotating Fiber-optic Gyro Inertial Navigation System. *Sensor Letters*, **10**, 1359–63.
- Yuan, B.L., Liao, D. and Han, S.L. (2012). Error Compensation of An Optical Gyro INS by Multi-axis Rotation. *Measurement Science and Technology*, **23**, 025102.
- Zhang, H., Wu, Y., Wu, W., Wu, M. and Hu, X. (2010). Improved Multi-position Calibration for Inertial Measurement Units. *Measurement Science and Technology*, **21**, 015107.